



Research Article

Cervical Cancer: Associations between Metabolic Parameters and Whole Lesion Histogram Analysis Derived from Simultaneous ^{18}F -FDG-PET/MRI

Hans-Jonas Meyer ¹, Sandra Purz,² Osama Sabri,² and Alexey Surov ¹

¹Department of Diagnostic and Interventional Radiology, University of Leipzig, Leipzig, Germany

²Department of Nuclear Medicine, University of Leipzig, Leipzig, Germany

Correspondence should be addressed to Hans-Jonas Meyer; jonas90.meyer@web.de

Received 17 April 2018; Revised 12 June 2018; Accepted 25 June 2018; Published 30 July 2018

Academic Editor: Elena Bonanno

Copyright © 2018 Hans-Jonas Meyer et al. This is an open access article distributed under the Creative Commons Attribution License, which permits unrestricted use, distribution, and reproduction in any medium, provided the original work is properly cited.

Multimodal imaging has been increasingly used in oncology, especially in cervical cancer. By using a simultaneous positron emission (PET) and magnetic resonance imaging (MRI, PET/MRI) approach, PET and MRI can be obtained at the same time which minimizes motion artefacts and allows an exact imaging fusion, which is especially important in anatomically complex regions like the pelvis. The associations between functional parameters from MRI and ^{18}F -FDG-PET reflecting different tumor aspects are complex with inconclusive results in cervical cancer. The present study correlates histogram analysis and ^{18}F -FDG-PET parameters derived from simultaneous FDG-PET/MRI in cervical cancer. Overall, 18 female patients (age range: 32–79 years) with histopathologically confirmed squamous cell cervical carcinoma were retrospectively enrolled. All 18 patients underwent a whole-body simultaneous ^{18}F -FDG-PET/MRI, including diffusion-weighted imaging (DWI) using b -values 0 and 1000 s/mm^2 . Apparent diffusion coefficient (ADC) histogram parameters included several percentiles, mean, min, max, mode, median, skewness, kurtosis, and entropy. Furthermore, mean and maximum standardized uptake values (SUV_{mean} and SUV_{max}), metabolic tumor volume (MTV), and total lesion glycolysis (TLG) were estimated. No statistically significant correlations were observed between SUV_{max} or SUV_{mean} and ADC histogram parameters. TLG correlated inversely with p25 ($r = -0.486, P = 0.041$), p75 ($r = -0.490, P = 0.039$), p90 ($r = -0.513, P = 0.029$), ADC median ($r = -0.497, P = 0.036$), and ADC mode ($r = -0.546, P = 0.019$). MTV also showed significant correlations with several ADC parameters: mean ($r = -0.546, P = 0.019$), p10 ($r = -0.473, P = 0.047$), p25 ($r = -0.569, P = 0.014$), p75 ($r = -0.576, P = 0.012$), p90 ($r = -0.585, P = 0.011$), ADC median ($r = -0.577, P = 0.012$), and ADC mode ($r = -0.597, P = 0.009$). ADC histogram analysis and volume-based metabolic ^{18}F -FDG-PET parameters are related to each other in cervical cancer.

1. Introduction

Cervical cancer is the third most commonly diagnosed cancer and the fourth leading cause of cancer death in females worldwide [1].

Magnetic resonance imaging (MRI) has been established as the best imaging modality for staging of cervical cancers due to its excellent soft tissue contrast [2]. Furthermore, MRI can provide information regarding tumor microstructure by diffusion-weighted imaging (DWI). The principle hypothesis is that DWI can quantify the free movement of protons (Brownian molecular movement) by using apparent diffusion coefficients (ADC) [3]. This movement is hindered

predominantly by cell membranes. In fact, previous studies showed that ADC inversely correlated with cell count in several malignant and benign lesions [4].

Another clinically important functional imaging modality is ^{18}F -fluorodeoxyglucose positron emission tomography (FDG-PET), which reflects tumor glucose-metabolism [5]. The FDG-uptake in tumor tissue is associated with the increased expression of glucose transporters (GLUT), mainly subtype GLUT-1 [6]. Clinically, ^{18}F -FDG-uptake is semi-quantified by standardized uptake values (SUV). Moreover, it has been shown that volume-based metabolic PET parameters, such as metabolic tumor volume (MTV) and total lesion glycolysis (TLG), might provide additional information

TABLE 1: Overview about published literature regarding correlation analysis between DWI and FDG-PET.

Author	Number of patients	Analyzed parameters	Correlation
Ho et al. [15]	33	ADC _{min, mean} , SUV _{max, mean}	No statistically significant correlations
Sun et al. [16]	35	ADC _{min, mean} , SUV _{max, mean}	No significant correlation between SUV _{max} and ADC _{min} ($r = -0.074, P = 0.501$) or between SUV _{mean} and ADC _{mean} ($r = -0.505, P = 0.201$) across all 35 primary tumors; for the 28 squamous cell carcinomas, there was also no significant correlation between SUV _{max} and ADC _{min} ($r = -0.363, P = 0.342$) or between SUV _{mean} and ADC _{mean} ($r = -0.354, P = 0.150$)
Wang et al. [35]	30	ADC _{min, mean} , SUV _{max, mean}	No statistically significant correlations between ADC and SUV fractions
Brandmaier et al. [10]	31 (14 primary, 17 recurrence)	ADC _{min, mean} , SUV _{max, mean}	SUV _{max} versus ADC _{min} ($r = -0.532, P = 0.05$) in primary tumors. Primary metastasis showed weak inverse correlations for SUV _{max} and ADC _{min} ($r = -0.362, P = 0.05$) and moderate correlations for SUV _{mean} and ADC _{min} ($r = -0.403, P = 0.03$)
Pinker et al. [36]	11	ADC _{mean} , SUV _{max}	No significant correlations
Surov et al. [14]	21	ADC _{min, mean, max} , SUV _{max, mean}	No significant correlations between ADC and SUV fractions
Lai et al. [37]	29	MTV, functional diffusion volume	Significant differences regarding MTV and functional diffusion volume derived from ADC maps

regarding tumor behavior [7]. MTV and TLG have been reported as possible prognostic factors, for example, for lung cancer or laryngeal carcinoma. In cervical cancer, for example, MTV was the only parameter to be of prognostic relevance in a multivariate analysis performed by Hong et al. [8].

Presumably, functional parameter derived from PET and from MRI, albeit reflecting slightly different tumor aspects, might be linked to each other [9]. As a hypothesis, a cell-rich tumor might also express more GLUT-transporters within their cell membranes, and hence, an association between ADC and SUV values might exist.

In fact, this was studied by various investigations in several different tumor entities like esophageal or breast cancer [9–13]. However, in a recent meta-analysis, comprising 35 studies, only a weak inverse correlation coefficient of $r = -0.30$ was identified over all various investigated tumors [9].

Regarding cervical cancer, there are inconclusive results [10, 14–16]. Table 1 summarizes the published data about reported correlations between ADC and SUV values. So, Brandmaier et al. identified an inverse correlation between SUV_{max} and ADC_{min} ($r = -0.532, P = 0.05$) [10], whereas most authors did not [14–16].

An emergent imaging analysis, namely, ADC histogram analysis, which is based on pixel distribution, is used to improve tumor heterogeneity in DWI-MRI assessment. Every voxel of a region of interest is issued into a histogram and thusly statistically information about the tumor is provided. Typically parameters are percentiles, median, mode, skewness, kurtosis, and entropy [17]. It is acknowledged that heterogeneity displayed by the histogram might be reflected by tumor microstructure heterogeneity, and therefore, a better reflection of tumor biology may be possible [17]. The histogram analysis approach has been applied in other tumors, for example, in prostate cancer. For example, Liu et al.

characterized histogram variables of ADC as predictors for the aggressiveness of prostate cancer [18]. In a study of Shindo et al., ADC histogram analysis has been described as helpful in differentiating pancreatic adenocarcinomas from neuroendocrine tumors [19]. Regarding cervical cancer, there are only few reports compared metabolic parameters of ¹⁸F-FDG-PET and ADC histogram analysis. For instance, Ueno et al. evaluated the prognostic value of SUV, MTV and TLG, and ADC histogram analysis for tumor response to therapy and event-free survival in patients with cervical cancer [20]. It has been shown that pretreatment volume-based metabolic ¹⁸F-FDG-PET parameters may have better potential than ADC histogram analysis for predicting treatment response and survival in these patients [20]. The main drawback of this study was that data from PET and MRI were obtained sequentially and not simultaneously; thus, the results of this study may have been influenced by this fact.

The aim of our study was to elucidate possible associations between ADC histogram-based parameters and ¹⁸F-FDG-PET parameters derived from simultaneous PET/MRI in cervical cancer.

2. Materials and Methods

This prospective study was approved by the local research ethics committee.

2.1. Patients. Overall, 18 female patients (age range: 32–79 years; mean age: 55.4 years) with histopathologically confirmed squamous cell cervical carcinoma were enrolled. Inclusion criteria were a staging investigating with a body simultaneous ¹⁸F-FDG-PET/MRI before any form of treatment.

Table 2 gives an overview about the patients and the different clinical pathological stages.

TABLE 2: Clinical data of the investigated patients.

Case	Age	Tumor grade	T stage	N stage	M stage
1	63	G2	2b	1	0
2	76	G3	4	0	0
3	65	G2	2b	0	0
4	63	G3	4	1	1
5	34	G3	2b	1	0
6	57	G2	4	1	1
7	53	G3	2b	0	0
8	32	G2	4	1	0
9	32	G2	2b	0	0
10	54	G2	3a	2	0
11	79	G3	4	1	0
12	52	G1	4	0	0
13	37	G3	2b	1	1
14	72	G3	4	0	0
15	46	G2	2b	1	1
16	71	G2	4	1	1
17	50	G2	2b	1	1
18	61	G2	4	1	0

2.2. PET/MRI. All 18 patients underwent a whole-body simultaneous ^{18}F -FDG-PET/MRI (Biograph mMR-Biograph, Siemens Healthcare Sector, Erlangen, Germany) which was performed from the upper thigh to the skull for 4 minutes per bed position. PET images were reconstructed using the iterative ordered subset expectation maximization algorithm with 3 iterations and 21 subsets, a Gaussian filter with 4 mm full width at half maximum (FWHM), and a 256×256 image matrix. Attenuation correction of the PET data was performed using a four-tissue (fat, soft tissue, air, and background) model attenuation map, which was generated from a Dixon-Vibe MR sequence according to previous description.

Radiotracer administration was performed intravenously after a fasting period of at least 6 hours with a body weight-adapted dose of ^{18}F -FDG (4 MBq/kg; range: 152–442 MBq; mean \pm std: 285 ± 70 MBq). PET/MRI image acquisition started on average 122 minutes after ^{18}F -FDG application. Due to radiotracer elimination via the urinary tract, which may influence evaluation of pelvic PET images, all patients received a bladder catheter prior to PET/MRI examination.

Image analysis was performed on the dedicated workstation of Hermes Medical Solutions, Sweden. For each tumor, maximum and mean SUV (SUV_{max} and SUV_{mean}), total lesion glycolysis (TLG), and metabolic tumor volume (MTV) were determined on PET images. MTV was defined as total tumor volume with an $\text{SUV} \geq 2.5$ and was calculated automatically. TLG was also calculated automatically by multiplying the MTV of the primary tumor by its SUV_{mean} .

In all cases, pelvic MRI was performed. Our investigation protocol included the following sequences: transverse T2 turbo spin echo (TSE) sequence (TR/TE: 5590/105), sagittal T2 TSE sequence (TR/TE: 4110/131), transverse T1 TSE sequence (TR/TE:1310/12), transverse T1 TSE after intravenous application of contrast medium (0.1 mmol/kg body weight Gadobutrol, Bayer Healthcare, Germany)

(TR/TE: 912/12), and sagittal postcontrast T1 TSE (TR/TE: 593/12). Additionally, diffusion-weighted imaging was performed using an echo-planar imaging (EPI) sequence (b_0 and $b1000 \text{ s/mm}^2$, TR/TE: 4900/105). Figure 1 shows an exemplary patient of our patient sample.

2.3. Histogram Analysis of ADC Values. Automatically generated ADC maps were transferred in DICOM format and processed offline with custom-made Matlab-based application (The Mathworks, Natick, MA) on a standard windows-operated system. The ADC maps were displayed within a graphical user interface (GUI), which enables the reader to scroll through the slices and draw a volume of interest (VOI) at the tumor’s boundary (whole-lesion measure). All measurements were performed by two authors blinded to each other (AS, HJM, 15 and 2 years of radiological experience). The ROIs were modified in the GUI and saved (in Matlab-specific format) for later processing. After setting the ROIs, following parameters were calculated and written in a spreadsheet format: ROI volume (cm^3), mean (ADC_{mean}), maximum (ADC_{max}), minimum (ADC_{min}), ADC median, 10th (p10 ADC), 25th (p25 ADC), 75th (p75 ADC), 90th (p90 ADC) percentile, and mode (ADC mode). Additionally, histogram-based characteristics of the ROI—kurtosis, skewness, and entropy—were calculated.

2.4. Statistical Analysis. Statistical analysis was performed using SPSS 23.0 (SPSS Inc, Chicago, IL). Collected data were evaluated by means of descriptive statistics. The data were not normally distributed according to Kolmogorow–Smirnow test. Therefore, Spearman’s correlation coefficient (ρ) was used to analyze associations between investigated parameters. Interreader variability was assessed with intraclass coefficients. P values < 0.05 were taken to indicate statistical significance.

3. Results

The investigated ADC histogram showed a good interreader variability, ranging from $\text{ICC} = 0.705$ for entropy to $\text{ICC} = 0.959$ for ADC median (Table 3).

Table 4 shows results of correlation analysis between the investigated PET and ADC parameters. No statistically significant correlations were observed between SUV_{max} or SUV_{mean} and ADC histogram parameters.

TLG correlated inversely with p25 ($r = -0.486, P = 0.041$), p75 ($r = -0.490, P = 0.039$), p90 ($r = -0.513, P = 0.029$), ADC median ($r = -0.497, P = 0.036$), and ADC mode ($r = -0.546, P = 0.019$). MTV also showed significant correlations with several ADC parameters as follows: mean ($r = -0.546, P = 0.019$), p10 ($r = -0.473, P = 0.047$), p25 ($r = -0.569, P = 0.014$), p75 ($r = -0.576, P = 0.012$), p90 ($r = -0.585, P = 0.011$), ADC median ($r = -0.577, P = 0.012$), and ADC mode ($r = -0.597, P = 0.009$). Finally, histogram-based parameters—skewness, kurtosis and entropy—did not correlate with PET parameters.

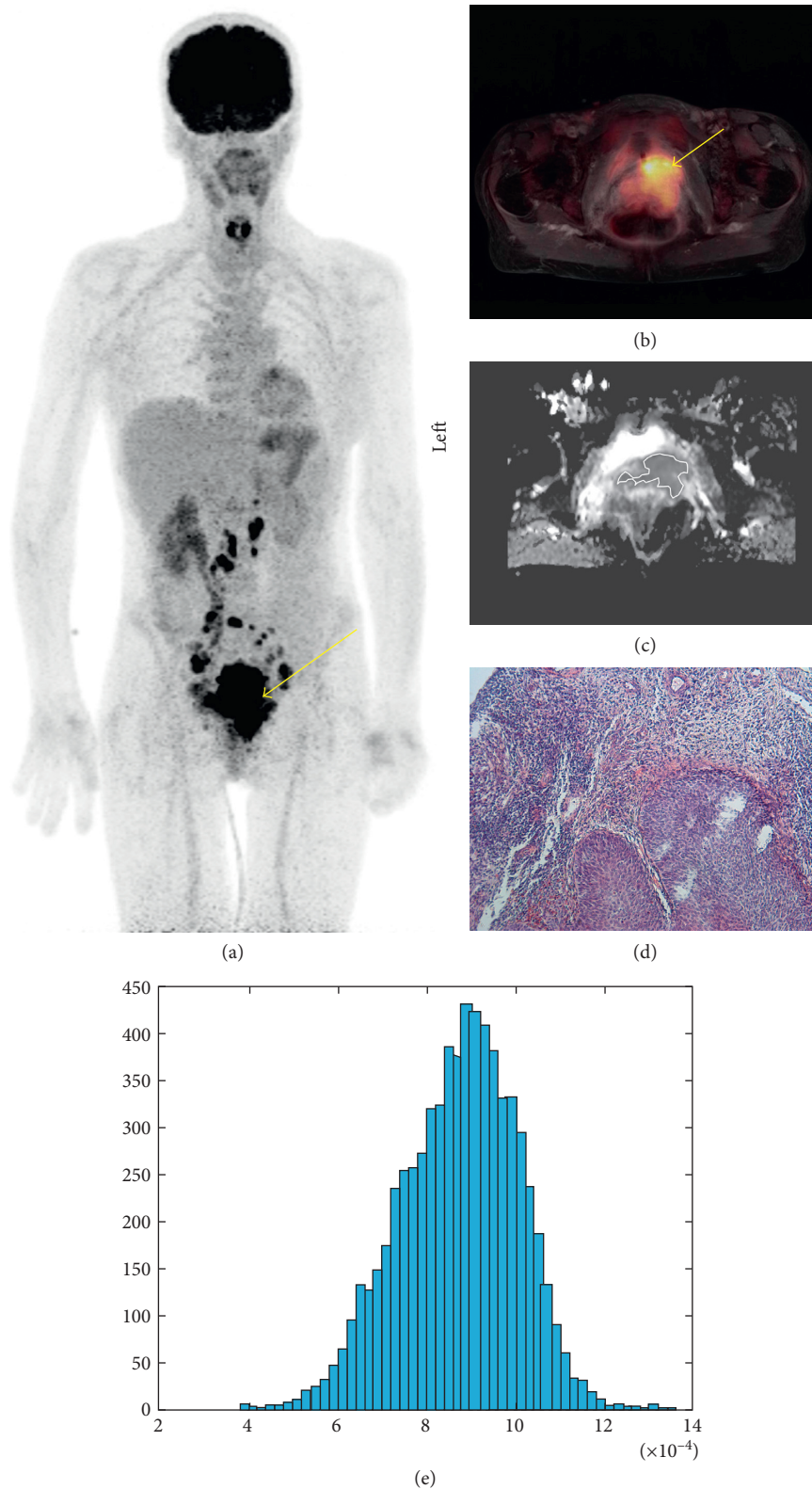


FIGURE 1: Imaging and histopathological findings in a case of cervical cancer. (a) ^{18}F -FDG-PET of a 57-year-old woman with locally advanced cervical cancer (arrow). (b) Fused ^{18}F -FDG-PET/MRI image demonstration of the metabolic active uterine cervical cancer (arrow). Calculated ^{18}F -FDG-PET parameters are as follows: $\text{SUV}_{\max} = 8.77$, $\text{SUV}_{\text{mean}} = 4.66$, $\text{SUV}_{\text{median}} = 4.32$, $\text{TLG} = 92.91$, and $\text{MTV} = 19.96$. (c) ADC map of the tumor with a ROI. (e) ADC histogram. The histogram analysis parameters ($\times 10^{-3} \text{ mm}^2 \cdot \text{s}^{-1}$) are as follows: $\text{ADC}_{\min} = 0.36$, $\text{ADC}_{\text{mean}} = 0.87$, $\text{ADC}_{\max} = 1.36$, $p_{10} = 0.7$, $p_{25} = 0.78$, $p_{75} = 0.96$, $p_{90} = 1.03$, median = 0.88, and mode = 0.93. Histogram-based characteristics are as follows: kurtosis = 2.96, skewness = -0.28, and entropy = 4.72. (d) Histopathological examination (hematoxylin and eosin-stained specimen) after tumor biopsy reveals a G2 cervical cancer.

TABLE 3: Interreader variability with intraclass coefficients of the investigated ADC parameters.

Parameter	ICC
ADC _{mean}	0.870
ADC _{min}	0.947
ADC _{max}	0.920
ADC P10	0.727
ADC P25	0.844
ADC P75	0.804
ADC P90	0.803
ADC median	0.959
ADC mode	0.917
Kurtosis	0.859
Skewness	0.792
Entropy	0.705

ICC, intraclass coefficient.

4. Discussion

To the best of our knowledge, this is the first study elucidating possible correlations between ADC histogram analysis and complex ¹⁸F-FDG-PET parameters derived from simultaneous PET/MRI in cervical cancer.

Pretherapeutic tumor staging in cervical cancer is of great importance. MRI is the best imaging modality to estimate regional tumor extent, with identification of tumor infiltration into the adjacent organs/tissues within the female pelvis [2]. Hybrid imaging, in terms of PET/CT, has been shown to be superior to other conventional imaging modalities (MRI, CT) for the identification of nodal or distant metastatic spread [21]. Consequently, the combination of both, namely, a simultaneous PET/MRI, has been described as valuable imaging modality for whole-body tumor staging of cervical cancer patients providing improved treatment planning when compared to MRI alone [22]. Furthermore, our own preliminary data show that simultaneous PET/MRI is a valuable imaging modality to reflect histopathologic parameters like cellularity and proliferation index in cervical cancer [14].

Additionally, functional MRI, as well as ¹⁸F-FDG-PET can provide information about tumor biology in a different fashion. ADC values derived from DWI are mainly influenced by cellularity, whereas SUV values derived from FDG-PET are mainly influenced by GLUT-1 overexpression within cell membranes and enhanced activity of tumor hexokinase [4, 14, 23].

Presumably, parameters from PET and MRI might be associated with each other due to the fact that a more cell-dense tumor also might express more GLUT-1 or may have an increased enzymatic activity [9]. However, a recent meta-analysis identified only a weak inverse correlation ($r = -0.30$) between SUV and ADC values pooling various tumors in oncologic imaging [9]. Regarding cervical cancer, the studies, which investigated associations between ADC and SUV values, showed inconclusive results [10, 14–16]. Only one study found an inverse correlation between SUV_{max} and ADC_{min} ($r = -0.532$) [10], whereas most authors could not identify linear correlations between these

parameters, indicating that they might reflect different tumor aspects [14–16].

The present study identified that several ADC histogram parameters were associated with volume-based metabolic PET parameters, namely, MTV and TLG. In good agreement with the literature, there were no correlations between ADC parameters and SUV values in the current patient sample. Therefore, our results suggest that ADC histogram analysis parameters and TLG and MTV are more sensitive to reflect relationships between ¹⁸F-FDG-PET and DWI than the widely used SUV and “conventional” ADC values. Furthermore, our study may explain negative results of the previous investigations. Moreover, in the present study, ADC values were obtained as a whole-lesion measurement, whereas in most studies [10, 14–16], only one slice was used for calculation and might therefore not be representative for the whole tumor. According to Kyriazi et al., whole-lesion measurement might be more beneficial than the conventional one slice approach since pixel-by-pixel ADC histograms through the entire tumor volume include different microenvironments of diffusivity, which may be masked by mean ADC analysis [24].

Furthermore, histogram-based analysis has been evaluated to have an excellent interobserver agreement [25, 26]. Additionally, it could clearly discriminate between tissue affected with cancer and physiological cervical tissue [25]. Finally, it could distinguish different FIGO stages: with increasing skewness, kurtosis, and entropy in the advanced stages indicating higher tumor heterogeneity in those lesions [26].

Interestingly, ADC histogram analysis parameters correlated with some histopathological features in cervical cancer. For example, entropy was associated with p53 expression [27]. Moreover, Meng et al. identified that ADC histogram parameters can predict tumor recurrence after radiochemotherapy with an area under the curve 0.85 [28]. In another study, it was identified that skewness and several percentiles derived from ADC maps were significantly different between squamous cell and adenocarcinomas of the uterine cervix and, therefore, ADC histogram analysis might aid in discrimination of the entities [29]. In fact, as reported previously, skewness was significantly higher for squamous cell carcinomas than adenocarcinomas and was higher in poorly differentiated tumors [29].

Regarding ¹⁸F-FDG-PET, pretreatment SUV_{max} and MTV have been reported to be associated with tumor prognosis [30, 31]. So MTV had a hazard ratio of 3.15 for disease-free survival [31], and SUV_{max} of the primary tumor was the only identified prognostic factor in a multivariate analysis [30]. Furthermore, TLG was also associated with the overall survival in locally advanced cervical cancer [32]. However, it might be of limited use for primary diagnosis in early stage carcinomas since ¹⁸F-FDG-PET only has little value in the routine pretreatment assessment in patients with early FIGO stages [33]. However, there are promising histopathological methods to better understand underlying microstructure changes, which can be displayed with PET imaging [34].

TABLE 4: Correlation between ADC histogram parameters and ^{18}F -FDG-PET parameters in cervical cancer. Spearman's rho correlation coefficient was used.

		SUV _{max}	SUV _{mean}	SUV _{median}	TLG	MTV
Mean ADC	<i>p</i> (rho)	-0.134	-0.215	-0.336	-0.461	-0.546
	<i>P</i>	0.595	0.392	0.173	0.054	0.019
Min ADC	<i>p</i> (rho)	-0.218	-0.213	-0.282	-0.219	-0.257
	<i>P</i>	0.385	0.396	0.257	0.382	0.303
Max ADC	<i>p</i> (rho)	-0.044	-0.166	-0.176	0.166	0.162
	<i>P</i>	0.861	0.510	0.484	0.510	0.521
P10 ADC	<i>p</i> (rho)	-0.183	-0.223	-0.332	-0.413	-0.473
	<i>P</i>	0.468	0.373	0.179	0.088	0.047
P25 ADC	<i>p</i> (rho)	-0.150	-0.214	-0.329	-0.486	-0.569
	<i>P</i>	0.553	0.395	0.182	0.041	0.014
P75 ADC	<i>p</i> (rho)	-0.142	-0.244	-0.354	-0.490	-0.576
	<i>P</i>	0.575	0.329	0.150	0.039	0.012
P90 ADC	<i>p</i> (rho)	-0.215	-0.275	-0.361	-0.513	-0.585
	<i>P</i>	0.392	0.270	0.142	0.029	0.011
Median ADC	<i>p</i> (rho)	-0.153	-0.244	-0.368	-0.497	-0.577
	<i>P</i>	0.544	0.329	0.133	0.036	0.012
Mode ADC	<i>p</i> (rho)	-0.225	-0.157	-0.261	-0.546	-0.597
	<i>P</i>	0.370	0.533	0.296	0.019	0.009
Kurtosis	<i>p</i> (rho)	-0.150	-0.148	-0.117	0.288	0.284
	<i>P</i>	0.553	0.559	0.645	0.247	0.254
Skewness	<i>p</i> (rho)	-0.095	-0.054	-0.004	0.149	0.142
	<i>P</i>	0.708	0.832	0.987	0.556	0.573
Entropy	<i>p</i> (rho)	0.071	-0.036	-0.049	0.084	0.172
	<i>P</i>	0.779	0.887	0.848	0.742	0.494

Significant correlations are highlighted in bold.

Overall, our report indicates that for further analyses about associations between DWI and PET and as well between PET, DWI, and histopathology in several tumors, ADC histogram analysis and volume-based metabolic PET parameters like TLG/MTV should be obtained.

There are several limitations of the present study to address. Firstly, it is a retrospective study with possible known bias. However, MRI and ^{18}F -FDG-PET were measured by two different readers, blinded to each other. Secondly, the patient sample is relatively small. Thirdly, only squamous cell carcinomas were evaluated.

In conclusion, the present study shows that ADC histogram analysis and volume-based metabolic ^{18}F -FDG-PET parameters are related to each other and might, therefore, reflect similar tumor behavior of cervical cancer. The next step would be to assess the value of these simultaneous PET/MRI parameters for predicting treatment response and survival in cervical cancer patients.

Abbreviations

MRI:	Magnetic resonance imaging
DWI:	Diffusion-weighted imaging
ADC:	Apparent diffusion coefficient
FDG-PET:	^{18}F -fluorodeoxyglucose positron emission tomography
TLG:	Total lesion glycolysis
MTV:	Mean tumor volume
GLUT:	Glucose transporters
SUV:	Standardized uptake value.

Data Availability

The anonymous patient data used to support the findings of this study are available from the corresponding author upon request.

Conflicts of Interest

The authors declare no conflicts of interest.

Authors' Contributions

Hans-Jonas Meyer, Alexey Surov, and Sandra Purz wrote the manuscript. Hans-Jonas Meyer and Alexey Surov performed histogram analysis. Sandra Purz and Osama Sabri performed PET analysis. Hans-Jonas Meyer performed the statistical analysis. All authors contributed equally to this work.

References

- [1] A. Jemal, F. Bray, M. M. Center et al., "Global cancer statistics," *Cancer Journal for Clinician*, vol. 61, no. 2, pp. 69–90, 2011.
- [2] E. Sala, S. Wakely, E. Senior, and D. Lomas, "MRI of malignant neoplasms of the uterine corpus and cervix," *American Journal of Roentgenology*, vol. 188, no. 6, pp. 1577–1587, 2007.
- [3] A. R. Padhani, G. Liu, D. M. Koh et al., "Diffusion-weighted magnetic resonance imaging as a cancer biomarker: consensus and recommendations," *Neoplasia: an International Journal for Oncology Research*, vol. 11, no. 2, pp. 102–125, 2009.

- [4] A. Surov, H. J. Meyer, and A. Wienke, "Correlation between apparent diffusion coefficient (ADC) and cellularity is different in several tumors: a meta-analysis," *Oncotarget*, vol. 8, no. 35, pp. 59492–59499, 2017.
- [5] H. H. Chung, S. Y. Kang, S. Ha et al., "Prognostic value of preoperative intratumoral FDG uptake heterogeneity in early stage uterine cervical cancer," *Journal of Gynecologic Oncology*, vol. 27, no. 2, p. e15, 2016.
- [6] M. S. Jo, O. H. Choi, D. S. Suh et al., "Correlation between expression of biological markers and Fluorodeoxyglucose uptake in endometrial cancer," *Oncology Research and Treatment*, vol. 37, no. 1-2, pp. 30–34, 2014.
- [7] H. J. Im, T. Bradshaw, M. Solaiyappan, and S. Y. Cho, "Current methods to define metabolic tumor volume in positron emission tomography: which one is better," *Nuclear Medicine and Molecular Imaging*, vol. 52, no. 1, pp. 5–15, 2018.
- [8] J. H. Hong, K. J. Min, J. K. Lee et al., "Prognostic value of the sum of metabolic tumor volume of primary tumor and lymph nodes using 18F-FDG PET/CT in patients with cervical cancer," *Medicine*, vol. 95, no. 9, article e2992, 2016.
- [9] G. Shen, H. Ma, B. Liu et al., "Correlation of the apparent diffusion coefficient and the standardized uptake value in neoplastic lesions: a meta-analysis," *Nuclear Medicine Communications*, vol. 38, no. 12, pp. 1076–1084, 2017.
- [10] P. Brandmaier, S. Purz, K. Bremicker et al., "Simultaneous [18F]FDG-PET/MRI: correlation of apparent diffusion coefficient (ADC) and standardized uptake value (SUV) in primary and recurrent cervical cancer," *PLoS One*, vol. 10, no. 11, Article ID e0141684, 2015.
- [11] L. Goense, S. E. Heethuis, P. S. N. van Rossum et al., "Correlation between functional imaging markers derived from diffusion-weighted MRI and 18F-FDG PET/CT in esophageal cancer," *Nuclear Medicine Communications*, vol. 39, no. 1, pp. 60–67, 2018.
- [12] K. A. Zukotynski, S. Vajapeyam, F. H. Fahey et al., "Correlation of 18F-FDG PET and MRI apparent diffusion coefficient histogram metrics with survival in diffuse intrinsic pontine glioma: a report from the pediatric brain tumor consortium," *Journal of Nuclear Medicine*, vol. 58, no. 8, pp. 1264–1269, 2017.
- [13] K. Kitajima, T. Yamano, K. Fukushima et al., "Correlation of the SUVmax of FDG-PET and ADC values of diffusion-weighted MR imaging with pathologic prognostic factors in breast carcinoma," *European Journal of Radiology*, vol. 85, no. 5, pp. 943–949, 2016.
- [14] A. Surov, H. J. Meyer, S. Schob et al., "Parameters of simultaneous 18F-FDG-PET/MRI predict tumor stage and several histopathological features in uterine cervical cancer," *Oncotarget*, vol. 8, no. 27, pp. 28285–28296, 2017.
- [15] K. C. Ho, G. Lin, J. J. Wang et al., "Correlation of apparent diffusion coefficients measured by 3T diffusion-weighted MRI and SUV from FDG PET/CT in primary cervical cancer," *European Journal of Nuclear Medicine and Molecular Imaging*, vol. 36, no. 2, pp. 200–208, 2009.
- [16] H. Sun, J. Xin, S. Zhang et al., "Anatomical and functional volume concordance between FDG PET, and T2 and diffusion-weighted MRI for cervical cancer: a hybrid PET/MR study," *European Journal of Nuclear Medicine and Molecular Imaging*, vol. 41, no. 5, pp. 898–905, 2014.
- [17] N. Just, "Improving tumour heterogeneity MRI assessment with histograms," *British Journal of Cancer*, vol. 111, no. 12, pp. 2205–2213, 2014.
- [18] W. Liu, X. H. Liu, W. Tang et al., "Histogram analysis of stretched-exponential and monoexponential diffusion-weighted imaging models for distinguishing low and intermediate/high gleason scores in prostate carcinoma," *Journal of Magnetic Resonance Imaging*, 2018, In press.
- [19] T. Shindo, Y. Fukukura, T. Umanodan et al., "Histogram analysis of apparent diffusion coefficient in differentiating pancreatic adenocarcinoma and neuroendocrine tumor," *Medicine*, vol. 95, no. 4, article e2574, 2016.
- [20] Y. Ueno, R. Lisbona, T. Tamada et al., "Comparison of FDG PET metabolic tumour volume versus ADC histogram: prognostic value of tumour treatment response and survival in patients with locally advanced uterine cervical cancer," *British Journal of Radiology*, vol. 90, no. 1075, article 20170035, 2017.
- [21] H. J. Choi, J. W. Roh, S. S. Seo et al., "Comparison of the accuracy of magnetic resonance imaging and positron emission tomography/computed tomography in the presurgical detection of lymph node metastases in patients with uterine cervical carcinoma: a prospective study," *Cancer*, vol. 106, no. 4, pp. 914–922, 2006.
- [22] T. Sarabhai, B. M. Schaarschmidt, A. Wetter et al., "Comparison of 18F-FDG PET/MRI and MRI for pre-therapeutic tumor staging of patients with primary cancer of the uterine cervix," *European Journal of Nuclear Medicine and Molecular Imaging*, vol. 45, no. 1, pp. 67–76, 2018.
- [23] H. J. Yang, W. J. Xu, Y. H. Guan et al., "Expression of Glut-1 and HK-II in pancreatic cancer and their impact on prognosis and FDG accumulation," *Translational Oncology*, vol. 9, no. 6, pp. 583–591, 2016.
- [24] S. Kyriazi, D. J. Collins, C. Messiou et al., "Metastatic ovarian and primary peritoneal cancer: assessing chemotherapy response with diffusion-weighted MR imaging—value of histogram analysis of apparent diffusion coefficients," *Radiology*, vol. 261, no. 1, pp. 182–192, 2011.
- [25] Y. Guan, W. Li, Z. Jiang et al., "Whole-lesion apparent diffusion coefficient-based entropy-related parameters for characterizing cervical cancers: initial findings," *Academic Radiology*, vol. 23, no. 12, pp. 1559–1567, 2016.
- [26] Y. Guan, W. Li, Z. Jiang et al., "Value of whole-lesion apparent diffusion coefficient (ADC) first-order statistics and texture features in clinical staging of cervical cancers," *Clinical Radiology*, vol. 72, no. 11, pp. 951–958, 2017.
- [27] S. Schob, H. J. Meyer, N. Pazaitis et al., "ADC histogram analysis of cervical cancer aids detecting lymphatic metastases—a preliminary study," *Molecular Imaging and Biology*, vol. 19, no. 6, pp. 953–962, 2017.
- [28] J. Meng, L. Zhu, L. Zhu et al., "Whole-lesion ADC histogram and texture analysis in predicting recurrence of cervical cancer treated with CCRT," *Oncotarget*, vol. 8, no. 54, pp. 92442–92453, 2017.
- [29] Y. Lin, H. Li, Z. Chen et al., "Correlation of histogram analysis of apparent diffusion coefficient with uterine cervical pathologic finding," *American Journal of Roentgenology*, vol. 204, no. 5, pp. 1125–1131, 2015.
- [30] S. Cima, A. M. Perrone, P. Castellucci et al., "Prognostic impact of pretreatment fluorodeoxyglucose positron emission tomography/computed tomography SUV_{max} in patients with locally advanced cervical cancer," *International Journal of Gynecological Cancer*, vol. 28, no. 3, pp. 575–580, 2018.
- [31] G. O. Chong, W. K. Lee, S. Y. Jeong et al., "Prognostic value of intratumoral metabolic heterogeneity on F-18 fluorodeoxyglucose positron emission tomography/computed tomography in locally advanced cervical cancer patients treated with concurrent chemoradiotherapy," *Oncotarget*, vol. 8, no. 52, pp. 90402–90412, 2017.

- [32] Y. Liang, X. Li, H. Wan et al., "Prognostic value of volume-based metabolic parameters obtained by 18F-FDG-PET/CT in patients with locally advanced squamous cell cervical carcinoma," *Journal of Computer Assisted Tomography*, vol. 42, no. 3, pp. 429–434, 2018.
- [33] D. O. Driscoll, D. Halpenny, C. Johnston et al., "18F-FDG-PET/CT is of limited value in primary staging of early stage cervical cancer," *Abdominal Imaging*, vol. 40, no. 1, pp. 127–133, 2015.
- [34] M. Scimeca, N. Urbano, R. Bonfiglio et al., "Management of oncological patients in the digital era: anatomic pathology and nuclear medicine teamwork," *Future Oncology*, vol. 14, no. 11, pp. 1013–1015, 2018.
- [35] P. Y. Wang, J. Xin, H. Z. Sun et al., "Observation on correlation of ADC value and SUV in primary squamous cell cervical cancer with hybrid 18F-FDG PET/MR," *Chinese Journal of Medical Imaging Technology*, vol. 30, pp. 603–607, 2014.
- [36] K. Pinker, P. Andrzejewski, P. Baltzer et al., "Multiparametric [18F]fluorodeoxyglucose/[18F]fluoromisonidazole positron emission tomography/magnetic resonance imaging of locally advanced cervical cancer for the non-invasive detection of tumor heterogeneity: a pilot study," *PLoS One*, vol. 11, no. 5, Article ID e0155333, 2016.
- [37] A. Y. T. Lai, J. A. U. Perucho, X. Xu et al., "Concordance of FDG PET/CT metabolic tumour volume versus DW-MRI functional tumour volume with T2-weighted anatomical tumour volume in cervical cancer," *BMC Cancer*, vol. 17, no. 1, p. 825, 2017.